

Flow of Ree-Eyring Fluids in Tubes of Elliptical Cross Sections

Taha Sochi (Contact: ResearchGate)

London, United Kingdom

Date of Publication: January 28, 2025

Abstract: In this paper we continue our previous investigation about the use of stress function in the flow of generalized Newtonian fluids through conduits of circular and non-circular (or/and multiply connected) cross sections where we inspect the flow of Ree-Eyring fluids in tubes of elliptical cross sections. We derive analytical expressions for the flow velocity profile and for the volumetric flow rate. The obtained analytical expressions were tested against the available analytical expressions for the special cases of Newtonian flow in circular tubes, Newtonian flow in elliptical tubes and Ree-Eyring flow in circular tubes and the results were identical. The obtained analytical expressions were also tested for sensible trends, tendencies and correlations and they passed all these tests.^[1]

Keywords: Ree-Eyring fluids, flow in elliptical tubes, non-Newtonian fluids, Newtonian fluids, generalized Newtonian fluids, shear thinning, rheology, fluid mechanics, fluid dynamics, stress function, flow velocity profile, volumetric flow rate, analytical expressions.

^[1] All symbols and abbreviations are defined in § [Nomenclature](#) in the back of this paper.

Contents

1	Introduction	3
2	Setting the Scene	4
3	Method and Formulation	4
4	Tests and Checks	8
4.1	Dimensional Checks	8
4.2	Velocity Profile Tests	9
4.3	Volumetric Flow Rate Tests	10
4.4	Trends, Tendencies and Correlations	10
4.5	Further Tests	11
5	Conclusions	11
	References	11
	Appendix	13
	Nomenclature	14

1 Introduction

Ree-Eyring fluid is a two-parameter model which describes time-independent shear-thinning yield-free non-Newtonian fluids. Although it is not a popular model it is relatively simple and hence it lends itself easily to analytical and numerical investigations (e.g. analytical expressions of flow velocity profile and volumetric flow rate for its flow through circular tubes and thin slits are easily derived). In fact, we conducted in the past a number of investigations about the flow of Ree-Eyring fluid in circular tubes and thin slits (see [1–3]) and this partly explains our interest in the flow of this model in other geometries (namely elliptical geometry in the present study).

In two of our previous investigations (see [4, 5]) we proposed using the stress function to develop a rather simple analytical and numerical strategies for obtaining the flow fields and attributes of generalized Newtonian fluid models in tubes of circular and non-circular (or with multiple connectivity) cross sectional geometries. In this paper we return to those investigations where we examine the flow of Ree-Eyring fluids in tubes of elliptical cross sectional geometry using the stress function approach that we proposed in those investigations (particularly in [5]).

In the present investigation we derive two analytical expressions for the flow velocity profile (one in polar coordinates and one in Cartesian coordinates) and another analytical expression for the volumetric flow rate. The derived analytical expressions were tested for certain limiting cases (namely the flow of Newtonian fluids in circular tubes, the flow of Newtonian fluids in elliptical tubes and the flow of Ree-Eyring fluids in circular tubes) and expected trends and correlations (such as the expected shear thinning behavior and its effect on the variation of flow velocity profile and volumetric flow rate) where these analytical expressions passed all these tests.

Our plan in this paper (following this introduction) is to prepare the scene for this investigation by stating the assumptions and conditions that apply to the fluid, flow and tube (see § 2). We then present the stress-function-based mathematical formulations which lead to the derivation of the aforementioned analytical expressions (see § 3). An outline of the tests and checks that were conducted to partially validate the derived formulae and rule out gross errors is then presented (see § 4). The paper is ended with a list of the main achievements and conclusions of this investigation (see § 5).

2 Setting the Scene

In this investigation we assume a laminar, isothermal, incompressible, rectilinear, steady-state, pressure-driven, fully-developed, creeping flow of purely-viscous, time-independent fluids characterized by the Ree-Eyring fluid model which is given by:

$$\tau = \tau_c \operatorname{arcsinh} \left(\frac{\mu_0 \gamma}{\tau_c} \right) \quad \rightarrow \quad \gamma = \frac{\tau_c}{\mu_0} \sinh \left(\frac{\tau}{\tau_c} \right) \quad (1)$$

The effects of external body forces, such as gravity, as well as the edge effects at the entry and exit zones of the tube are assumed non-existing or negligible. Dependencies of the attributes of fluid and flow on physical factors like temperature, which are not related to fluid deformation, are also ignored assuming fixed conditions or negligible contribution from these factors (noting that this applies to the physique of tube wall and shape as well). The flow is also assumed to be in purely shear mode with no extensional contributions. Regarding the velocity boundary conditions, a no-slip at the tube wall is assumed and hence a zero velocity condition at the fluid-solid interface is maintained. Regarding the pressure boundary conditions we assume constant time-independent pressure at the inlet and outlet of the tube.

As for the type of tube, we use a pipe of elliptical cross sectional shape with semi-major axis a and semi-minor axis b where a uniform pressure drop is imposed along the tube length dimension which defines the flow direction. The pressure is supposed to be constant temporally and spatially at each cross section perpendicular to the flow direction where the pressure is assumed to be a sole function of the axial dimension in the flow direction (i.e. the pressure linearly varies along the axial dimension and hence the pressure gradient as a function of the axial dimension is constant). The pipe is assumed to be straight with a cross sectional area that is constant in shape and size along the flow axial direction. We also assume rigid mechanical properties of the tube wall and hence the tube wall is not deformable under the considered range of pressure (as well as any other physical conditions such as temperature as hinted earlier). In fact, we should assume that the tube wall and shape are inert in their physical and geometrical properties to all the involved physical conditions and variations of the flow system and its ambient conditions.

3 Method and Formulation

As indicated already, the proposal of the use of stress function is fully explained and justified in [4, 5] and hence we do not repeat. So, all we need to do here is to continue

from the final stage that we reached in [5] where we identified the components of the stress function (i.e. the Newtonian stress function which we assume here to be universal) for a number of geometries including the elliptical geometry which is the subject of interest in the present investigation.

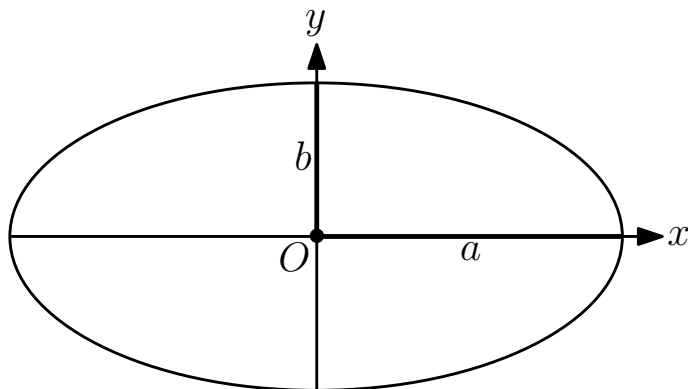


Figure 1: The setting of the elliptical cross section of the tube where a and b represent the semi-major and semi-minor axes and O is the origin of coordinates.

For a tube with an elliptical cross section (centered on the origin of coordinates) of semi-major axis a along the x axis and semi-minor axis b along the y axis (refer to Figure 1) and whose central axis is oriented along the z axis, the magnitudes of the components of the stress function are given by:

$$\tau_{xz} = \frac{\partial p}{\partial z} \frac{b^2 x}{a^2 + b^2} = Ab^2 x \quad (2)$$

$$\tau_{yz} = \frac{\partial p}{\partial z} \frac{a^2 y}{a^2 + b^2} = Aa^2 y \quad (3)$$

where:

$$A = \frac{\partial p}{\partial z} \frac{1}{a^2 + b^2} \quad (4)$$

A 2D visualization of the stress function for an elliptical tube is given in the upper frame of Figure 2, while a 3D visualization of this stress function is given in the lower frame of this Figure.

Now, on the x axis of an elliptical cross section of semi-axes a and b we have $\tau_{yz} = 0$ and hence $\tau = \tau_{xz}$ where the magnitude of τ_{xz} is given by Eq. 2. Therefore, the rate of shear strain on the x axis is given by (see Eq. 1):

$$\gamma = \frac{\tau_c}{\mu_0} \sinh \left(\frac{\tau_{xz}}{\tau_c} \right) \quad (5)$$

$$= \frac{\tau_c}{\mu_0} \sinh \left(\frac{Ab^2x}{\tau_c} \right) \quad (6)$$

where $0 \leq x \leq a$. On substituting $\gamma = dv/dx$ in the last equation we get:

$$\frac{dv}{dx} = \frac{\tau_c}{\mu_0} \sinh \left(\frac{Ab^2x}{\tau_c} \right) \quad (7)$$

Now, if v_X symbolizes the fluid velocity at $x = X$ on the x axis (where $0 \leq X \leq a$) then by integrating the velocity along the x axis (starting from $x = a$, where $v_a = 0$ according to the no-slip at wall condition, and ending at $x = X$) we get:

$$v_X = \int_a^X \frac{dv}{dx} dx \quad (8)$$

$$= \int_a^X \frac{\tau_c}{\mu_0} \sinh \left(\frac{Ab^2x}{\tau_c} \right) dx \quad (9)$$

$$= \left[\frac{\tau_c^2}{Ab^2\mu_0} \cosh \left(\frac{Ab^2x}{\tau_c} \right) \right]_a^X \quad (10)$$

$$= \frac{\tau_c^2}{Ab^2\mu_0} \left[\cosh \left(\frac{Ab^2X}{\tau_c} \right) - \cosh \left(\frac{Ab^2a}{\tau_c} \right) \right] \quad (11)$$

Now, a given point of coordinates (x, y) within the ellipse should belong to a given ellipse of the same eccentricity as the original ellipse (i.e. of semi-axes a and b) and with a given semi-major axis X , and hence this point should be on the velocity contour of v_X , i.e. $v(x, y) = v_X$. So, all we need to identify $v(x, y)$ is to identify its corresponding v_X , and this should be easily done by mapping the point (x, y) on the point $(X, 0)$ where we exploit the basic mathematical formulae and relationships of ellipse, that is:

$$e = \sqrt{1 - (b/a)^2} \quad (12)$$

$$x = r \cos \phi \quad y = r \sin \phi \quad (13)$$

$$r = \sqrt{x^2 + y^2} \quad (14)$$

$$r = X \sqrt{\frac{1 - e^2}{1 - (e \cos \phi)^2}} \quad (15)$$

$$X = r \sqrt{\frac{1 - (e \cos \phi)^2}{1 - e^2}} \quad (16)$$

On obtaining X from (x, y) as outlined in the above equations we simply substitute from Eq. 16 into Eq. 11 to get our analytical expression of v as a function of (r, ϕ) , that

is:

$$v(r, \phi) = v_X \quad (17)$$

$$v(r, \phi) = \frac{\tau_c^2}{Ab^2\mu_0} \left[\cosh \left(\frac{Ab^2r \sqrt{1 - (e \cos \phi)^2}}{\tau_c \sqrt{1 - e^2}} \right) - \cosh \left(\frac{Ab^2a}{\tau_c} \right) \right] \quad (18)$$

If we substitute $r = \sqrt{x^2 + y^2}$ and $\cos \phi = x/\sqrt{x^2 + y^2}$ in this expression and simplify we get v as a function of (x, y) , that is:

$$v(x, y) = \frac{\tau_c^2}{Ab^2\mu_0} \left[\cosh \left(\frac{Ab^2 \sqrt{x^2 - e^2x^2 + y^2}}{\tau_c \sqrt{1 - e^2}} \right) - \cosh \left(\frac{Ab^2a}{\tau_c} \right) \right] \quad (19)$$

Regarding the volumetric flow rate Q we have (where we use the polar version of the velocity profile, i.e. Eq. 18):

$$Q = \frac{\tau_c^2}{Ab^2\mu_0} \int_{\phi=0}^{\phi=2\pi} \int_{r=0}^{r=b/\sqrt{1-(e \cos \phi)^2}} \left[\cosh \left(\frac{Ab^2r \sqrt{1 - (e \cos \phi)^2}}{\tau_c \sqrt{1 - e^2}} \right) - \cosh \left(\frac{Ab^2a}{\tau_c} \right) \right] r dr d\phi \quad (20)$$

$$= \frac{\tau_c^2}{Ab^2\mu_0} \int_{\phi=0}^{\phi=2\pi} \int_{r=0}^{r=b/\sqrt{1-(e \cos \phi)^2}} \left[r \cosh \left(\frac{Ab^2r \sqrt{1 - (e \cos \phi)^2}}{\tau_c \sqrt{1 - e^2}} \right) - r \cosh \left(\frac{Ab^2a}{\tau_c} \right) \right] dr d\phi \quad (21)$$

$$= \frac{\tau_c^2}{Ab^2\mu_0} \int_{\phi=0}^{\phi=2\pi} \left[\frac{\frac{Ab^2 \sqrt{1-(e \cos \phi)^2}}{\tau_c \sqrt{1-e^2}} r \sinh \left(\frac{Ab^2r \sqrt{1-(e \cos \phi)^2}}{\tau_c \sqrt{1-e^2}} \right) - \cosh \left(\frac{Ab^2r \sqrt{1-(e \cos \phi)^2}}{\tau_c \sqrt{1-e^2}} \right)}{\frac{A^2b^4[1-(e \cos \phi)^2]}{\tau_c^2(1-e^2)}} - \frac{r^2}{2} \cosh \left(\frac{Ab^2a}{\tau_c} \right) \right]_{r=0}^{r=b/\sqrt{1-(e \cos \phi)^2}} d\phi \quad (22)$$

$$= \frac{\tau_c^2}{Ab^2\mu_0} \int_{\phi=0}^{\phi=2\pi} \left[\frac{\frac{Ab^3}{\tau_c \sqrt{1-e^2}} \sinh \left(\frac{Ab^3}{\tau_c \sqrt{1-e^2}} \right) - \cosh \left(\frac{Ab^3}{\tau_c \sqrt{1-e^2}} \right)}{\frac{A^2b^4[1-(e \cos \phi)^2]}{\tau_c^2(1-e^2)}} - \frac{b^2 \cosh \left(\frac{Ab^2a}{\tau_c} \right)}{2[1-(e \cos \phi)^2]} + \frac{\tau_c^2(1-e^2)}{A^2b^4[1-(e \cos \phi)^2]} \right] d\phi \quad (23)$$

$$= \frac{4\tau_c^2}{Ab^2\mu_0} \left[\frac{\frac{Ab^3}{\tau_c\sqrt{1-e^2}} \sinh\left(\frac{Ab^3}{\tau_c\sqrt{1-e^2}}\right) - \cosh\left(\frac{Ab^3}{\tau_c\sqrt{1-e^2}}\right)}{\frac{A^2b^4}{\tau_c^2(1-e^2)}} - \frac{b^2 \cosh\left(\frac{Ab^2a}{\tau_c}\right)}{2} + \frac{\tau_c^2(1-e^2)}{A^2b^4} \right] \int_{\phi=0}^{\phi=\pi/2} \frac{d\phi}{1-(e\cos\phi)^2} \quad (24)$$

$$= \frac{4\tau_c^2}{Ab^2\mu_0} \left[\frac{\frac{Ab^3}{\tau_c\sqrt{1-e^2}} \sinh\left(\frac{Ab^3}{\tau_c\sqrt{1-e^2}}\right) - \cosh\left(\frac{Ab^3}{\tau_c\sqrt{1-e^2}}\right)}{\frac{A^2b^4}{\tau_c^2(1-e^2)}} - \frac{b^2 \cosh\left(\frac{Ab^2a}{\tau_c}\right)}{2} + \frac{\tau_c^2(1-e^2)}{A^2b^4} \right] \frac{\arctan\left(\frac{\tan(\pi/2)}{\sqrt{1-e^2}}\right)}{\sqrt{1-e^2}} \quad (25)$$

$$Q = \frac{4\tau_c^4\sqrt{1-e^2}}{A^3b^6\mu_0} \left[\frac{Ab^3}{\tau_c\sqrt{1-e^2}} \sinh\left(\frac{Ab^3}{\tau_c\sqrt{1-e^2}}\right) - \cosh\left(\frac{Ab^3}{\tau_c\sqrt{1-e^2}}\right) - \frac{A^2b^6}{2\tau_c^2(1-e^2)} \cosh\left(\frac{Ab^2a}{\tau_c}\right) + 1 \right] \arctan\left(\frac{\tan(\pi/2)}{\sqrt{1-e^2}}\right) \quad (26)$$

where A is given by Eq. 4.

4 Tests and Checks

A number of tests and checks on the analytical expressions for the flow velocity profile (i.e. Eqs. 18 and 19) and the volumetric flow rate (i.e. Eq. 26) were conducted to partially validate the derived expressions and exclude gross errors. A sample of these tests and checks are outlined in the following subsections.

4.1 Dimensional Checks

Dimensional inspection of the analytical expressions for the flow velocity profile (i.e. Eqs. 18 and 19) reveals that they have the physical dimension of length over time which is the physical dimension of velocity as it should be. Similarly, dimensional inspection of the analytical expression for the volumetric flow rate (i.e. Eq. 26) reveals that it has the physical dimension of volume over time which is the physical dimension of volumetric flow rate as it should be.

4.2 Velocity Profile Tests

Thorough investigation to the flow velocity profile of the derived formulae (i.e. Eqs. 18 and 19) in the following three special cases (which represent three common types of flow in tubes) was conducted:^[2]

1. Circular Newtonian (i.e. Poiseuille): the velocity profile for the flow of Newtonian fluids through a circular tube of radius R is given by (see [6]):

$$v(r) = \frac{R^2 - r^2}{4\mu} \nabla P \quad (27)$$

The results of the derived analytical expressions for the flow velocity profile (i.e. Eqs. 18 and 19 with $a = b = R$, $\mu_0 = \mu$, $\partial p/\partial z = \nabla P$ and large τ_c) were compared to the results of this formula (i.e. Eq. 27) and they were identical. A sample of these comparisons is given in Figure 3.

2. Elliptic Newtonian: the velocity profile for the flow of Newtonian fluids through a tube of elliptical cross section with semi-axes a and b is given by (see [7, 8]):

$$v(x, y) = \frac{a^2 b^2}{2\mu(a^2 + b^2)} \left(1 - \frac{x^2}{a^2} - \frac{y^2}{b^2} \right) \nabla P \quad (28)$$

The results of the derived analytical expressions for the flow velocity profile (i.e. Eqs. 18 and 19 with $\mu_0 = \mu$, $\partial p/\partial z = \nabla P$ and large τ_c) were compared to the results of this formula (i.e. Eq. 28) and they were identical. A sample of these comparisons is given in Figure 4.

3. Circular Ree-Eyring: the velocity profile for the flow of Ree-Eyring fluids through a circular tube of radius R is given by (see § Appendix):

$$v(r) = \frac{2\tau_c^2}{\mu_0 \nabla P} \left[\cosh \left(\frac{\nabla P}{2\tau_c} R \right) - \cosh \left(\frac{\nabla P}{2\tau_c} r \right) \right] \quad (29)$$

The results of the derived analytical expressions for the flow velocity profile (i.e. Eqs. 18 and 19 with $a = b = R$ and $\partial p/\partial z = \nabla P$) were compared to the results of this formula (i.e. Eq. 29) and they were identical. A sample of these comparisons is given in Figure 5.

^[2] The Taylor expansion of \sinh is given by:

$$\sinh x = x + \frac{x^3}{3!} + \frac{x^5}{5!} + \dots$$

Therefore, the Newtonian model approximates the Ree-Eyring model when $x \gg \frac{x^3}{3!}$, i.e. $\frac{\tau}{\tau_c} \gg \frac{\tau^3}{6\tau_c^3}$ (see Eq. 1).

4.3 Volumetric Flow Rate Tests

Thorough investigation to the volumetric flow rate of the derived formula (i.e. Eq. 26) in the following three special cases (which represent three common types of flow in tubes) was conducted:

1. Circular Newtonian (i.e. Poiseuille): the volumetric flow rate for the flow of Newtonian fluids through a circular tube of radius R is given by (see [6]):

$$Q = \frac{\pi R^4}{8\mu} \nabla P \quad (30)$$

The results of the derived analytical expression for the volumetric flow rate (i.e. Eq. 26 with $a = b = R$, $\mu_0 = \mu$, $\partial p/\partial z = \nabla P$ and large τ_c) were compared to the results of this formula (i.e. Eq. 30) and they were identical. A sample of these comparisons is given in Figure 6.

2. Elliptic Newtonian: the volumetric flow rate for the flow of Newtonian fluids through a tube of elliptical cross section with semi-axes a and b is given by (see [7, 8]):

$$Q = \frac{\pi a^3 b^3}{4\mu(a^2 + b^2)} \nabla P \quad (31)$$

The results of the derived analytical expression for the volumetric flow rate (i.e. Eq. 26 with $\mu_0 = \mu$, $\partial p/\partial z = \nabla P$ and large τ_c) were compared to the results of this formula (i.e. Eq. 31) and they were identical. A sample of these comparisons is given in Figure 7.

3. Circular Ree-Eyring: the volumetric flow rate for the flow of Ree-Eyring fluids through a circular tube of radius R is given by (see [1, 3]):

$$Q = \frac{\pi R^3 \tau_c}{\tau_w^3 \mu_0} \left[(\tau_c \tau_w^2 + 2\tau_c^3) \cosh\left(\frac{\tau_w}{\tau_c}\right) - 2\tau_c^2 \tau_w \sinh\left(\frac{\tau_w}{\tau_c}\right) - 2\tau_c^3 \right] \quad (32)$$

The results of the derived analytical expression for the volumetric flow rate (i.e. Eq. 26 with $a = b = R$ and $\partial p/\partial z = \nabla P$) were compared to the results of this formula (i.e. Eq. 32) and they were identical. A sample of these comparisons is given in Figure 8.

4.4 Trends, Tendencies and Correlations

Trends, tendencies and correlations of the derived formulae for the flow velocity profile (i.e. Eqs. 18 and 19) and for the volumetric flow rate (i.e. Eq. 26) were investigated and they were found sensible and inline with expectations. For example:

1. The effect of varying the characteristic shear stress τ_c on shear thinning (and hence

- on the flow velocity profile and volumetric flow rate) was investigated and found to be logical and sensible. This also applies to the variation of the low-shear viscosity μ_0 .
2. The effect of varying the tube geometry (such as the tube size and eccentricity) was investigated and found to be logical and sensible.
 3. The effect of varying the pressure gradient was investigated and found to be logical and sensible.

4.5 Further Tests

We are not aware of any other theoretical or experimental proposals or results that we can compare with our results in this study. Therefore, we look for other researchers in this field to assess and test our proposals and results theoretically and empirically.

5 Conclusions

We outline in the following points the main achievements and conclusions of the present paper:

1. In this investigation we derived three analytical formulae that represent the flow velocity profile (i.e. Eqs. 18 and 19) and the volumetric flow rate (i.e. Eq. 26) for the flow of Ree-Eyring fluids in tubes of elliptical cross sections.
2. We tested the convergence of these formulae to three special cases representing three types of flow (i.e. the flow of Newtonian fluids in circular tubes, the flow of Newtonian fluids in elliptical tubes, and the flow of Ree-Eyring fluids in circular tubes) and the formulae passed these tests.
3. We inspected trends, tendencies and correlations indicated by these formulae and the results of all these inspections were sensible and as expected.
4. If there is any doubt about the validity of the proposals and formulae that we presented and derived in this investigation (i.e. mainly the proposal of stress function and Eqs. 18, 19 and 26), there should be no doubt about the value of these proposals and formulae as each one of these three formulae which are derived from the proposal of stress function represents three types of flow (i.e. circular Newtonian, elliptical Newtonian and circular Ree-Eyring) simultaneously, and this condensation of formulation should be very useful theoretically and practically (e.g. in modeling and coding).

References

- [1] T. Sochi. Variational approach for the flow of Ree-Eyring and Casson fluids in pipes. 2015. arXiv:1412.6209.
- [2] T. Sochi. Further validation to the variational method to obtain flow relations for generalized Newtonian fluids. *Korea-Australia Rheology Journal*, 27(2):113–124, 2015.
- [3] T. Sochi. Variational approach for resolving the flow of generalized Newtonian fluids in circular pipes and plane slits. 2015. arXiv:1503.01262.
- [4] T. Sochi. Using the stress function in the flow of generalized Newtonian fluids through pipes and slits. 2015. arXiv:1503.07600.
- [5] T. Sochi. Using the stress function in the flow of generalized Newtonian fluids through conduits with non-circular or multiply connected cross sections. 2015. arXiv:1509.01648.
- [6] T. Sochi. Using the Euler-Lagrange variational principle to obtain flow relations for generalized Newtonian fluids. *Rheologica Acta*, 53(1):15–22, 2014.
- [7] F.M. White. *Viscous Fluid Flow*. McGraw Hill Inc., second edition, 1991.
- [8] J. Lekner. Viscous flow through pipes of various cross-sections. *European Journal of Physics*, 28(3):521–527, 2007.

Appendix

We derive in this appendix the velocity profile for the flow of Ree-Eyring fluids (see Eq. 1) through a circular tube of radius R .^[3]

$$\tau(r) = \frac{\nabla P}{2} r \quad (33)$$

$$\gamma = \frac{\tau_c}{\mu_0} \sinh\left(\frac{\tau}{\tau_c}\right) \quad (34)$$

$$\frac{dv}{dr} = \frac{\tau_c}{\mu_0} \sinh\left(\frac{\tau}{\tau_c}\right) \quad (35)$$

$$v(r) = \int_R^r \frac{dv}{dr} dr \quad (36)$$

$$v(r) = \int_R^r \frac{\tau_c}{\mu_0} \sinh\left(\frac{\tau}{\tau_c}\right) dr \quad (37)$$

$$v(r) = \frac{\tau_c}{\mu_0} \int_R^r \sinh\left(\frac{\nabla P}{2\tau_c} r\right) dr \quad (38)$$

$$v(r) = \frac{2\tau_c^2}{\mu_0 \nabla P} \left[\cosh\left(\frac{\nabla P}{2\tau_c} r\right) \right]_R^r \quad (39)$$

$$v(r) = \frac{2\tau_c^2}{\mu_0 \nabla P} \left[\cosh\left(\frac{\nabla P}{2\tau_c} R\right) - \cosh\left(\frac{\nabla P}{2\tau_c} r\right) \right] \quad (40)$$

^[3] We note that r is used as a limit and as a variable. However, this should not cause any confusion. We also reversed the sign of the final expression to get the magnitude (which is what we are interested in).

Nomenclature

2D, 3D	two dimensional, three dimensional
a, b	semi-major and semi-minor axes of ellipse (m)
e	eccentricity of ellipse ()
Eq., Eqs.	Equation, Equations
p	pressure (Pa)
Q	volumetric flow rate ($\text{m}^3 \cdot \text{s}^{-1}$)
r	radius (m)
R	tube radius (m)
r, ϕ	polar coordinates (m,)
v	fluid velocity ($\text{m} \cdot \text{s}^{-1}$)
v_X	fluid velocity value on the coordinates $x = X$ and $y = 0$ ($\text{m} \cdot \text{s}^{-1}$)
$v(r, \phi)$	fluid velocity as a function of polar coordinates ($\text{m} \cdot \text{s}^{-1}$)
$v(x, y)$	fluid velocity as a function of Cartesian coordinates ($\text{m} \cdot \text{s}^{-1}$)
x, y, z	coordinate variables (usually spatial coordinates)
∇P	pressure gradient ($\text{Pa} \cdot \text{m}^{-1}$)
γ	rate of shear strain (s^{-1})
μ	Newtonian viscosity (Pa.s)
μ_0	low-shear viscosity in Ree-Eyring model (Pa.s)
τ	shear stress (Pa)
τ_c	characteristic shear stress in Ree-Eyring model (Pa)
τ_w	shear stress at tube wall [$= \frac{R}{2} \nabla P$] (Pa)
τ_{xz}, τ_{yz}	shear stress components (Pa)

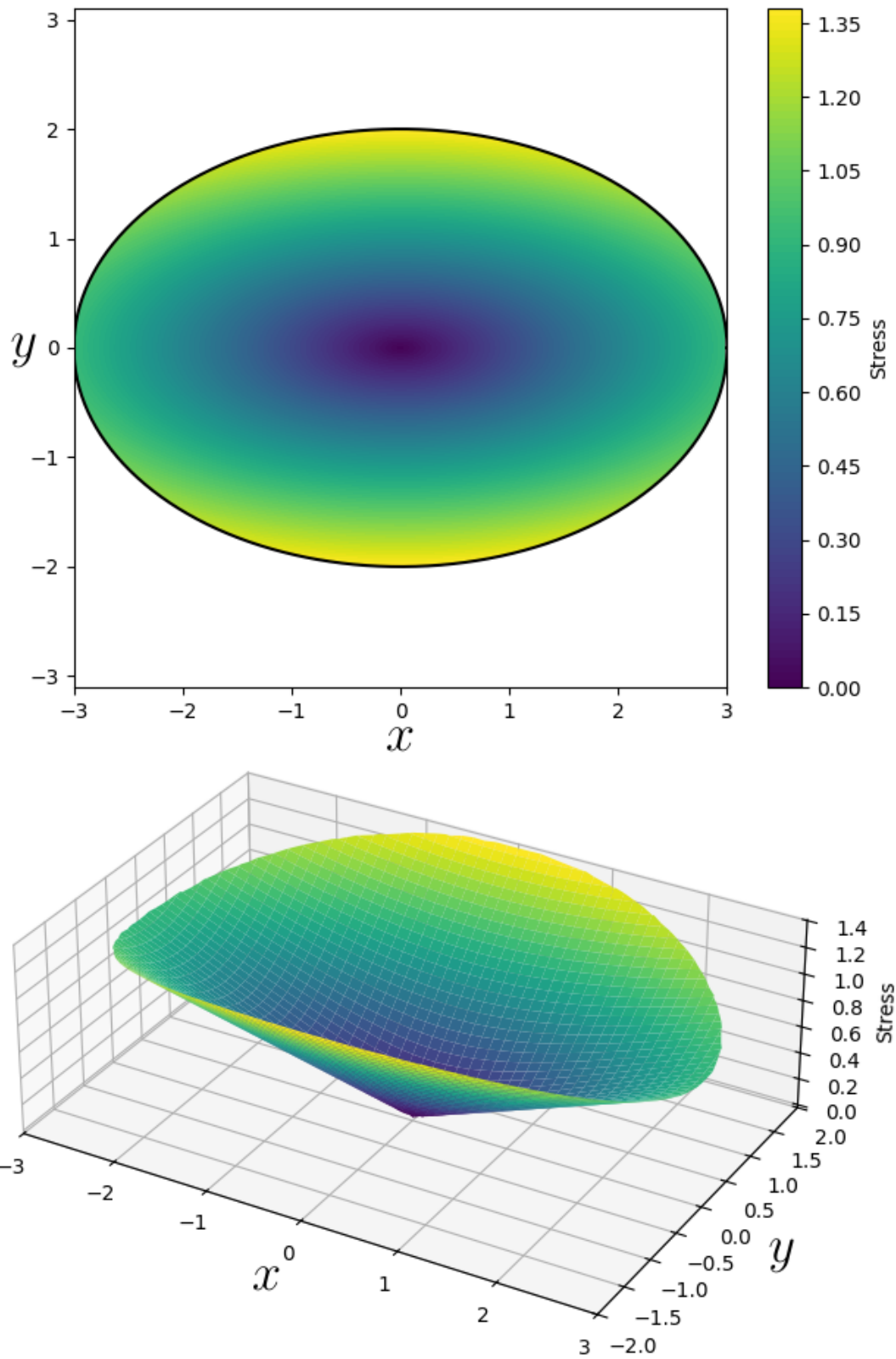


Figure 2: 2D and 3D graphic illustrations of the stress function for an elliptical tube with $a = 3$ and $b = 2$ with a typical pressure gradient.

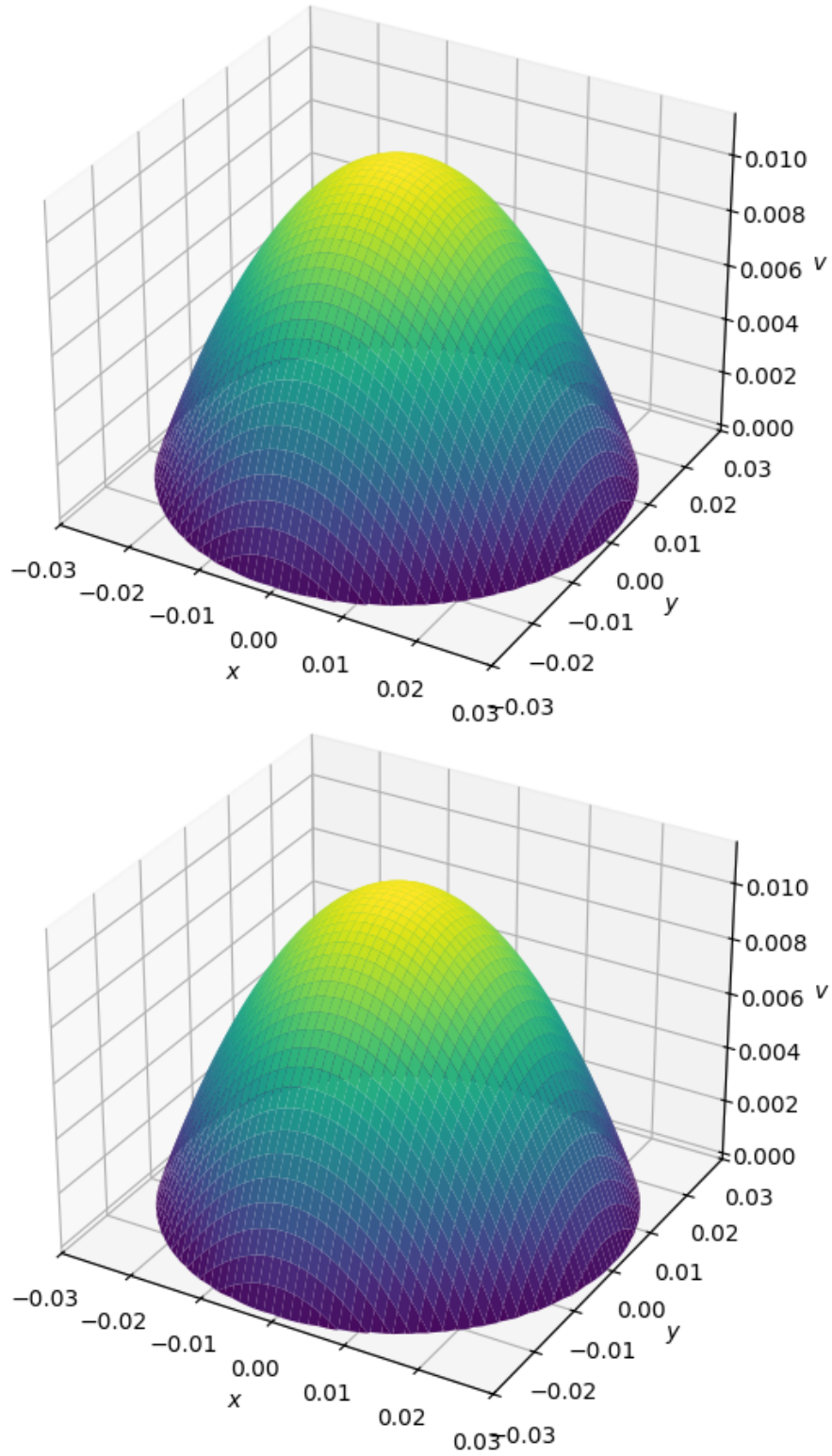


Figure 3: A 3D plot of the velocity profile for the Newtonian flow in circular tube as given by Eq. 27 (upper frame) and the Ree-Eyring flow in elliptical tube as given by Eq. 19 (lower frame) with $a = b = R = 0.03$, $\mu_0 = \mu = 0.2$, $\tau_c = 40$ and $\partial p/\partial z = \nabla P = 10$. As we see, the two plots are identical.

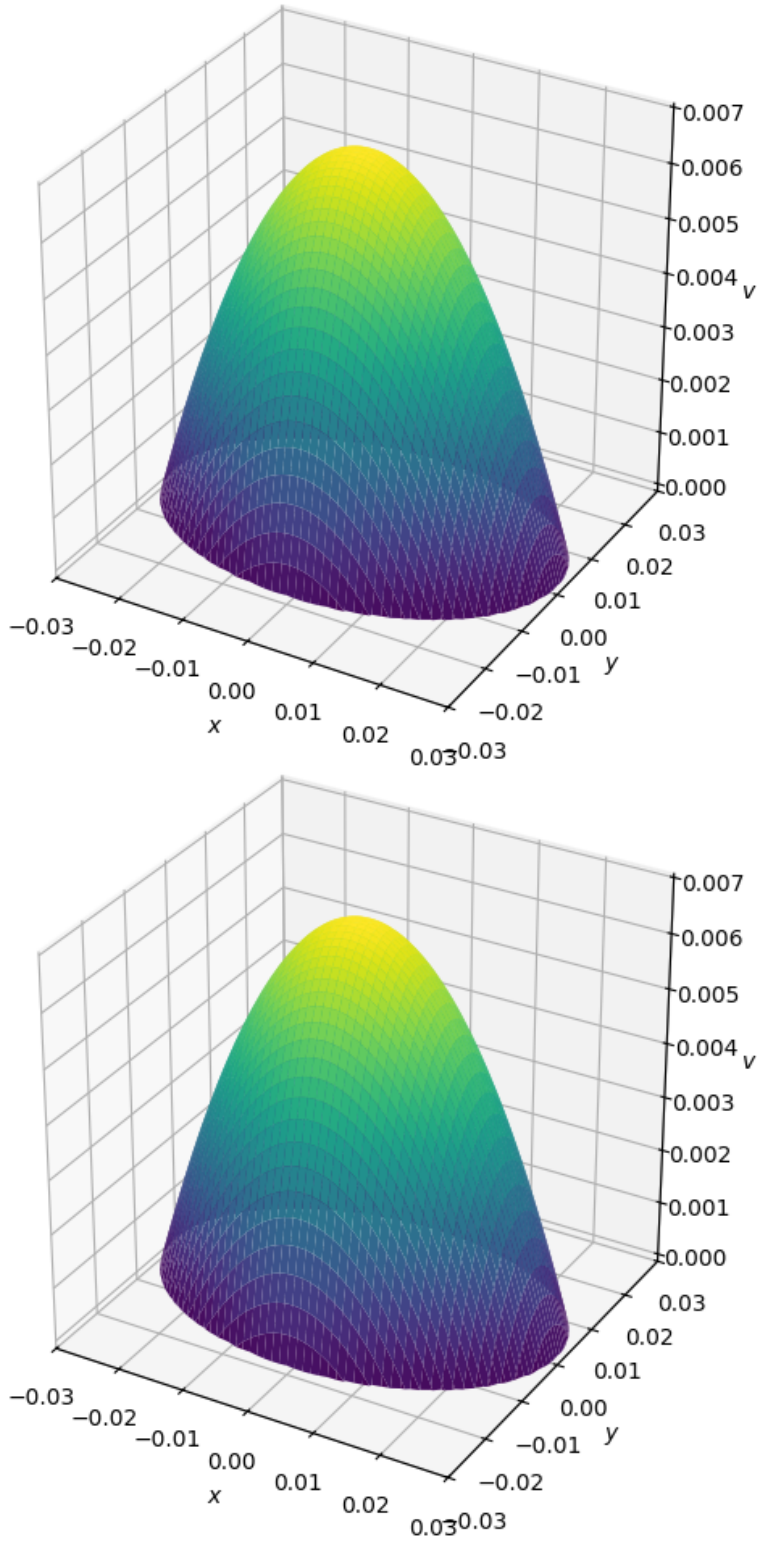


Figure 4: A 3D plot of the velocity profile for the Newtonian flow in elliptical tube as given by Eq. 28 (upper frame) and the Ree-Eyring flow in elliptical tube as given by Eq. 19 (lower frame) with $a = 0.03$, $b = 0.02$, $\mu_0 = \mu = 0.2$, $\tau_c = 40$ and $\partial p/\partial z = \nabla P = 10$. As we see, the two plots are identical.

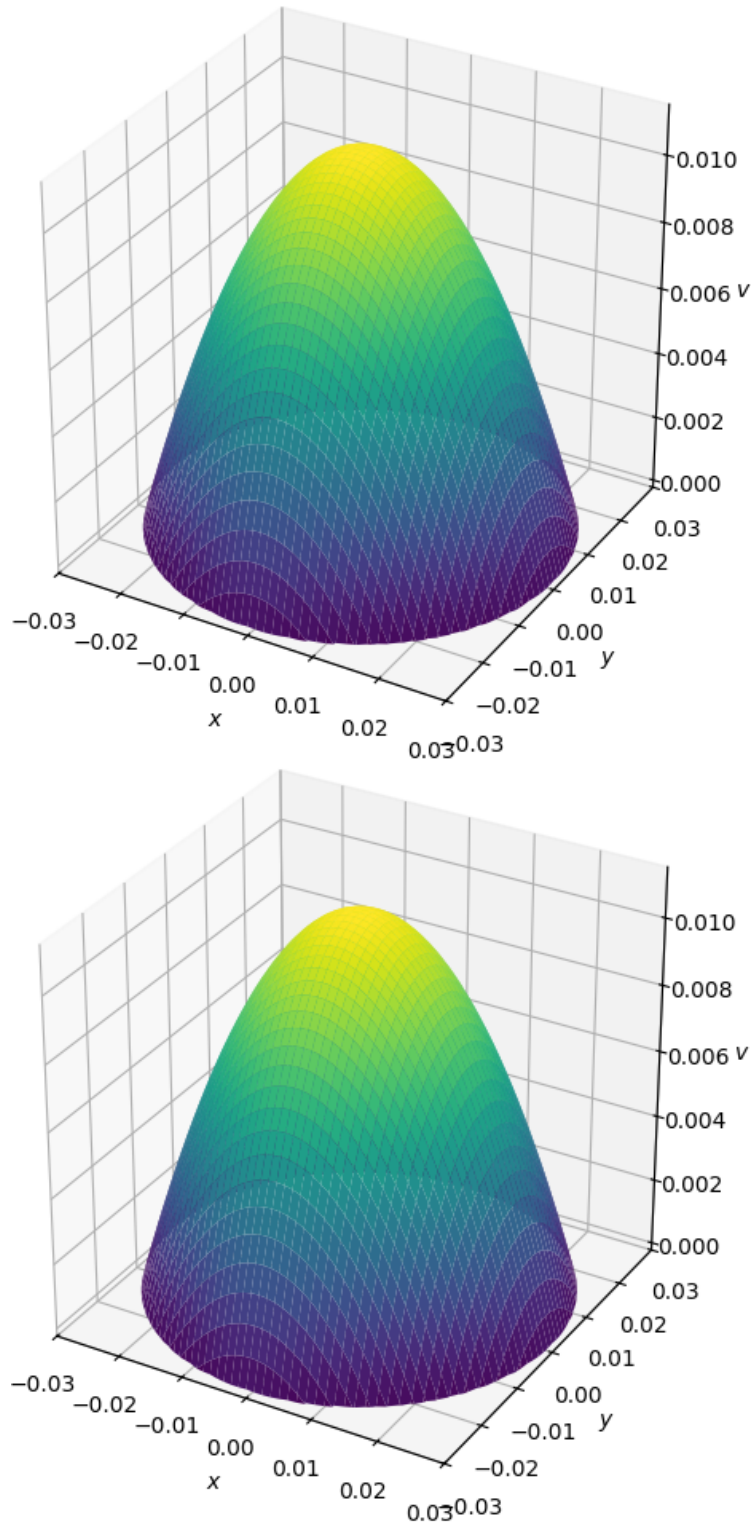


Figure 5: A 3D plot of the velocity profile for the Ree-Eyring flow in circular tube as given by Eq. 29 (upper frame) and the Ree-Eyring flow in elliptical tube as given by Eq. 19 (lower frame) with $a = b = R = 0.03$, $\mu_0 = 0.2$, $\tau_c = 2$ and $\partial p/\partial z = \nabla P = 10$. As we see, the two plots are identical.

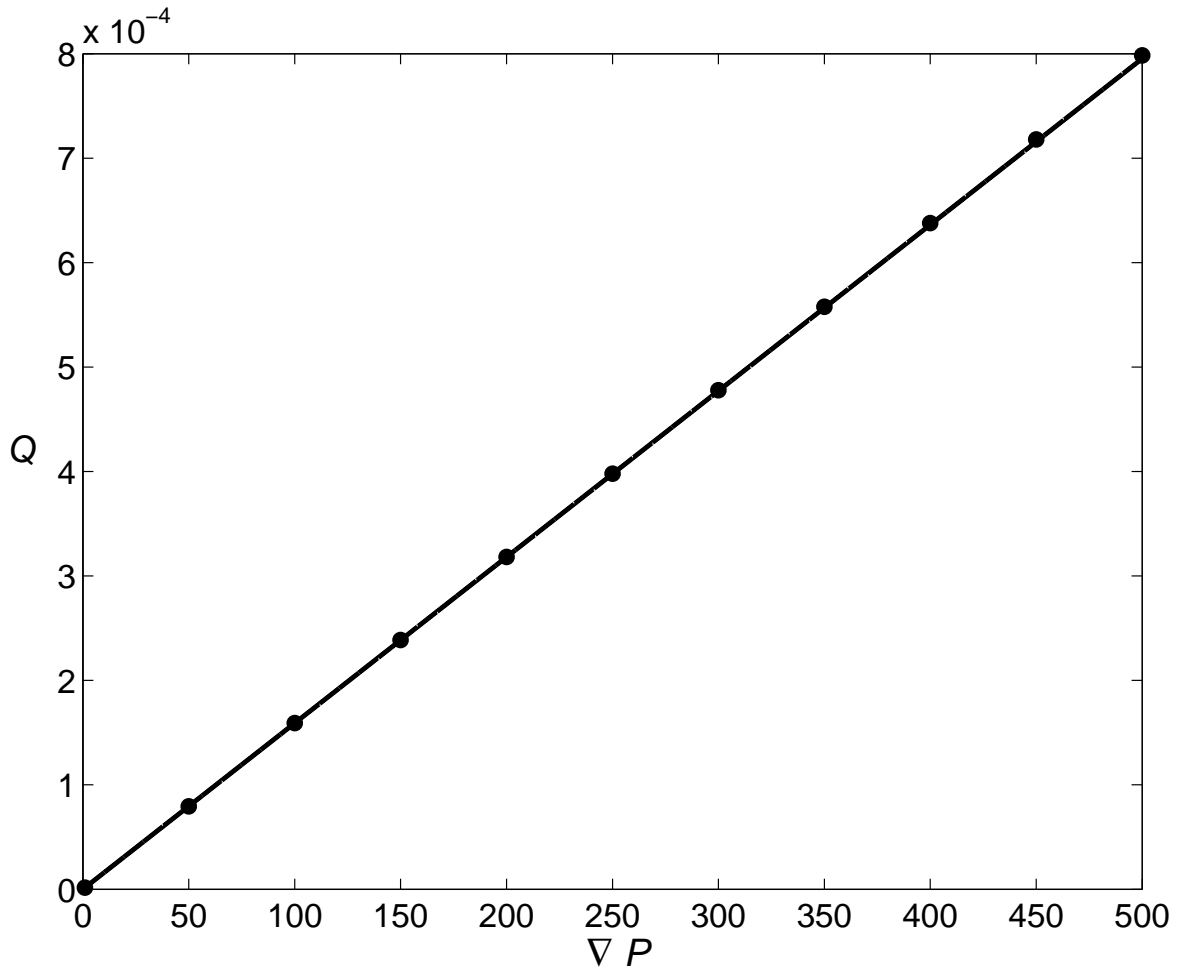


Figure 6: A plot of the volumetric flow rate for the Newtonian flow in circular tube as given by Eq. 30 (continuous line) and the Ree-Eyring flow in elliptical tube as given by Eq. 26 (circles) with $a = b = R = 0.03$, $\mu_0 = \mu = 0.2$ and $\tau_c = 40$.

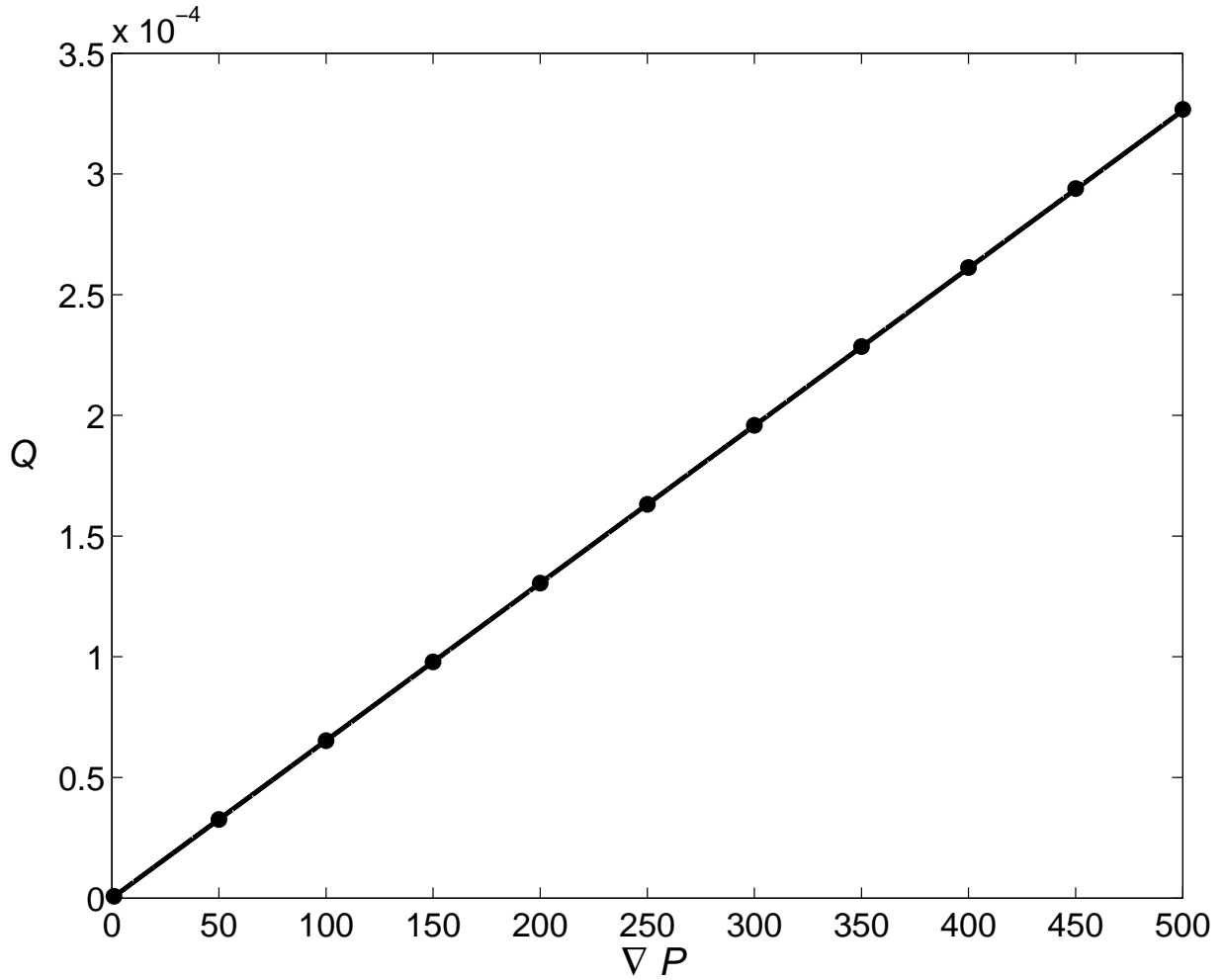


Figure 7: A plot of the volumetric flow rate for the Newtonian flow in elliptical tube as given by Eq. 31 (continuous line) and the Ree-Eyring flow in elliptical tube as given by Eq. 26 (circles) with $a = 0.03$, $b = 0.02$, $\mu_0 = \mu = 0.2$ and $\tau_c = 40$.

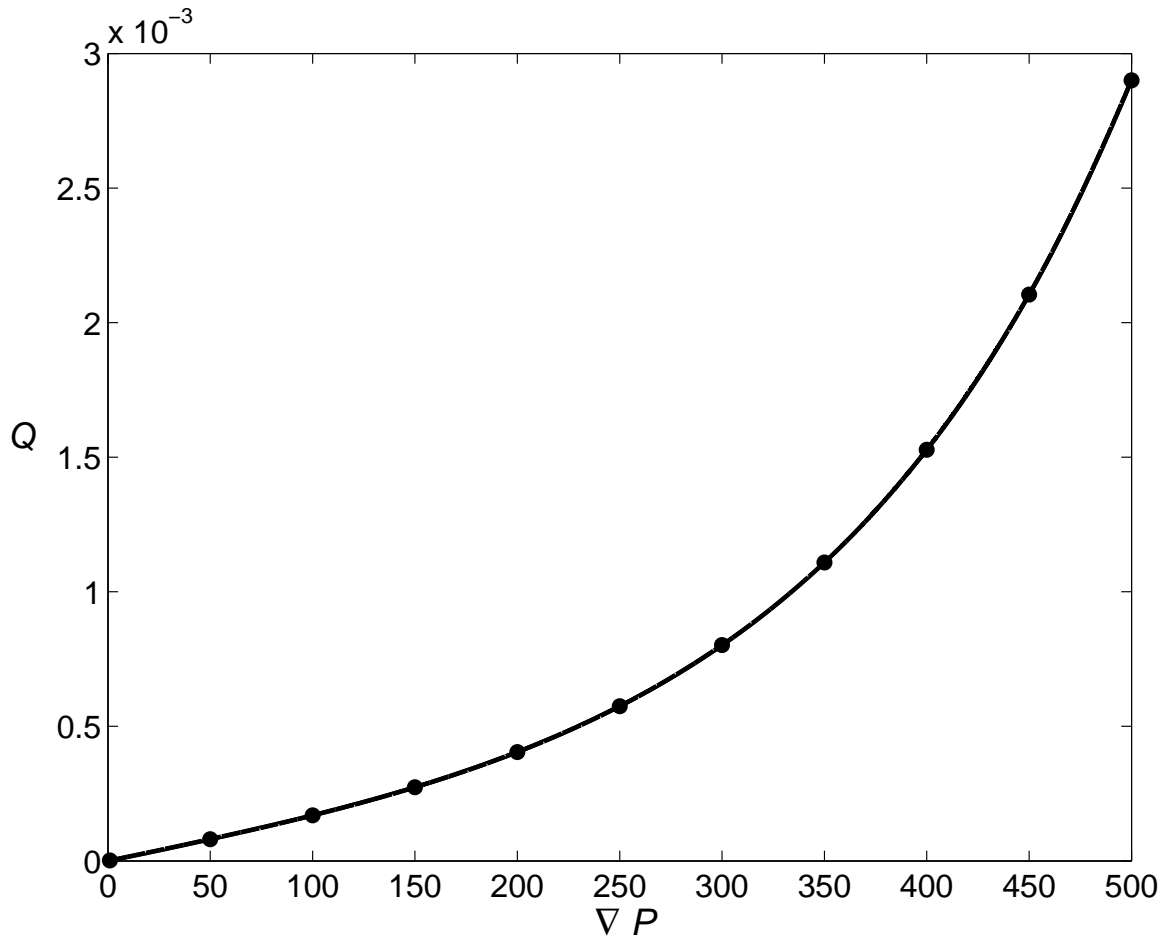


Figure 8: A plot of the volumetric flow rate for the Ree-Eyring flow in circular tube as given by Eq. 32 (continuous line) and the Ree-Eyring flow in elliptical tube as given by Eq. 26 (circles) with $a = b = R = 0.03$, $\mu_0 = 0.2$ and $\tau_c = 2$.